HEFAT2010
7th International Conference on Heat Transfer, Fluid Mechanics and Thermodynamics
19-21 July 2010
Antalya, Turkey

Study on the prediction of the inner wall surface geometry of a two-layer-wall furnace by an inverse process combined with grey theory

Chin-Ru Su[1], Chieh-Li Chen[2]*
[1]Department of Mechanical and Computer-Aided Engineering,
National Formosa University, Yunlin, Taiwan, ROC
[2]Department of Aeronautics and Astronautics,
National Cheng Kung University, Tainan, Taiwan, ROC
chiehli@mail.ncku.edu.tw

ABSTRACT

In this work the inner wall surface geometry of a two-layer-wall furnace system is estimated using inverse process method combined with grey prediction model. In estimating process a virtual area extended from the inner surface of furnace wall is used for analysis. The heat conduction equation and the boundary condition are first discretized by finite difference method to form a linear matrix equation; the inverse model is then optimized by linear least-squares error method and the temperatures of virtual boundary are obtained from a few of measured temperatures in furnace wall using the linear inverse model; and finally the temperature distribution of system is got by direct process and the inner surface geometry of furnace wall can be estimated accordingly. The result shows that using inverse process combined with grey prediction model the geometry can be exactly estimated from relatively small number of measured temperatures. Moreover, the effects of measurement error, location and number of measured points on the estimation for inner surface geometry of furnace wall are discussed in detail.

INTRODUCTION

In inverse heat conduction problem, if the temperatures at some appropriate points on the surface or inside the solid are measured by an infrared optical thermometer or a thermo-couple, the data can then be used to find the initial values and boundary conditions or to analyze some significant parameters, such as thermal conductivity [1], surface heat flux [2]. As for the estimate of undetermined geometry of the boundary by inverse process, a general method was first developed in 1986 by Hsieh [3]. This method can also be applied for the estimation of non-linear geometry. A three dimensional geometry was successfully predicted by the finite element methods proposed by Met [4]. In 1997, Huang [5] estimated an irregular boundary using a boundary element approach by both conjugate gradient and Levenberg-Marquardt methods.

Grey theory was pioneered by professor Deng in 1982[6]. The key technique for grey prediction is to obtain a new series from an original series using accumulated generating operation (AGO), then to form a differential equation and get its solution from the new series, and finally to obtain the prediction result for the original series by means of inverse accumulated generating operation (IAGO). Chen and Tien [7,8] estimated the prediction model parameters using deterministic convergence scheme and proposed a method for prediction, namely, deterministic grey dynamic model (DGDM). There is a transfer function existing between the input and output series for this model, so the prediction accuracy can be largely promoted. In this work, DGDM is combined with the inverse process for estimating the inner wall surface geometry of a two-layer-wall furnace in order to reduce the number of really measured points and promote the work efficiency.

PHYSICAL MODEL AND GOVERNING EQUATIONS

A two-dimensional furnace of two layer walls with different materials was taken as the system for study in this work, as shown in Fig.1. The radius of the furnace outer surface, $\bar{r}_o$, and the boundary between the outer and inner layer walls, $\bar{r}_b$, are constant. The radius of the furnace inner surface, $\bar{r}_i$, varies with θ ,i.e. $\bar{r}_i = f(\theta)$, which is the unknown geometry to be estimated. For establishing a physical model for this work some assumptions were made as follows:

1. The temperature inside the furnace, $\bar{T}_i$, is at steady state in long operation period.
2. The temperature at the furnace outer surface is $\bar{T}_o$.
3. The surrounding temperature around furnace is $\bar{T}_\infty$.
4. The thermal conductivity are constant, k_i and k_o for the inner and outer layer walls of the furnace, respectively.
5. The contact thermal resistance between the inner and outer layer walls of the furnace is neglected due to their compactness.
6. The heat transfer coefficient, h, is also constant.

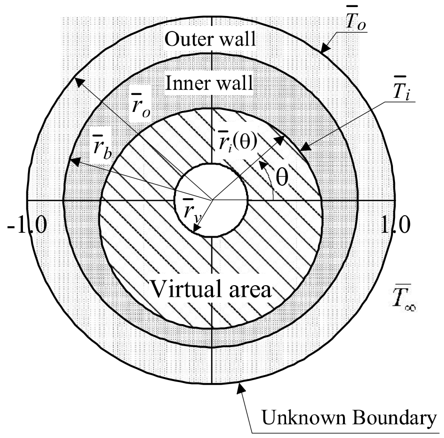

Fig.1 A two-dimensional system of two layer furnace walls with a sinusoidal inner surface containing a virtual area.

Therefore, the governing equation for this system can be represented as follows:

$$\frac{1}{\overline{r}}\frac{\partial}{\partial \overline{r}}\left(\overline{r}\frac{\partial \overline{T}(\overline{r},\theta)}{\partial \overline{r}}\right)+\frac{1}{\overline{r}^2}\frac{\partial^2 \overline{T}(\overline{r},\theta)}{\partial \theta^2}=0 \qquad (1)$$

The associated boundary conditions are given as

$$\overline{T}(\overline{r},\theta)=\overline{T}_i \qquad \overline{r}=\overline{r}_i \qquad (2)$$

$$-k_o\frac{\partial \overline{T}(\overline{r},\theta)}{\partial \overline{r}}=h(\overline{T}_o-\overline{T}_\infty) \qquad \overline{r}=\overline{r}_o \qquad (3)$$

For the boundary between the inner and outer layer of the furnace walls is

$$\overline{T}_{ib}(\overline{r}_b,\theta)=\overline{T}_{ob}(\overline{r}_b,\theta) \qquad \overline{r}=\overline{r}_b \qquad (4)$$

$$k_i\left(\frac{\partial \overline{T}(\overline{r},\theta)}{\partial \overline{r}}\right)_i=k_o\left(\frac{\partial \overline{T}(\overline{r},\theta)}{\partial \overline{r}}\right)_o \qquad \overline{r}=\overline{r}_b \qquad (5)$$

where $\overline{T}_{ib}$ and $\overline{T}_{ob}$ are the temperatures of the boundaries for the inner and outer layer walls of the furnace, respectively.

Since the temperature varies periodically for θ with a period 2π, one can have

$$\overline{T}(\overline{r},\theta)=\overline{T}(\overline{r},\theta+2\pi) \qquad (6)$$

The dimensionless parameters are taken as

$$r=\frac{\overline{r}}{\overline{r}_o} \qquad r_o=\frac{\overline{r}_o}{\overline{r}_o}=1 \qquad r_b=\frac{\overline{r}_b}{\overline{r}_o} \qquad r_i=\frac{\overline{r}_i}{\overline{r}_o}$$

$$r_v=\frac{\overline{r}_v}{\overline{r}_o} \qquad T=\frac{\overline{T}-\overline{T}_\infty}{\overline{T}_i-\overline{T}_\infty} \qquad Bi=\frac{h\overline{r}_o}{k_o} \qquad (7)$$

The governing equation and boundary conditions Eqs. (1) - (6), can be transformed into a dimensionless form as the following by means of Eq. (7).

$$\frac{1}{r}\frac{\partial}{\partial r}\left(r\frac{\partial T(r,\theta)}{\partial r}\right)+\frac{1}{r^2}\frac{\partial^2 T(r,\theta)}{\partial \theta^2}=0 \qquad (8)$$

$$T(r,\theta)=1 \qquad r=r_i \qquad (9)$$

$$\frac{\partial T(r,\theta)}{\partial r}=-Bi\,T(r,\theta) \qquad r=r_o=1 \qquad (10)$$

$$T_{ib}(r_b,\theta)=T_{ob}(r_b,\theta) \qquad r=r_b \qquad (11)$$

$$k_i\left(\frac{\partial T(r,\theta)}{\partial r}\right)_i=k_o\left(\frac{\partial T(\overline{r},\theta)}{\partial r}\right)_o \qquad r=r_b \qquad (12)$$

$$T(r,\theta)=T(r,\theta+2\pi) \qquad (13)$$

where Bi is Biot number and $Bi=0.225$, $k_{io}=k_i/k_o=0.125$, $r_b=0.8$ is used in this work.

In the inverse process for predicting the unknown boundary geometry, $r_i=r_i(\theta)$, a virtual area with an inner boundary, $r=r_v$ and $r_v<r_i(\theta)$, is introduced as shown in Fig.1. The inner surface of furnace wall has a sinusoidal shape and can be expressed by the following function.

$$r_i(\theta)=0.6-0.1\sin\theta \qquad (14)$$

NUMERICAL METHOD

A. Direct problem

The temperature measurement was not actually performed in this work. Therefore, it is necessary by the direct problem to get the temperatures of the outer surface and the inside of the furnace wall and then provide some temperatures of measured points for the inverse process. The finite-difference method was first used to discretize the governing equation and boundary condition of Eqs. (8)-(13). The result was shown as follows:

$$\frac{1}{(\Delta r)^2}(T_{j-1,k}-2T_{j,k}+T_{j+1,k})+\frac{1}{r_j}\frac{1}{2\Delta r}(T_{j+1,k}-T_{j-1,k})$$

$$+\frac{1}{r_j^2}\frac{1}{(\Delta\theta)^2}(T_{j,k-1}-2T_{j,k}+T_{j,k+1})=0 \qquad (15)$$

$$T_{j,k}=1 \qquad r=r_i \qquad (16)$$

$$T_{jb,k}=\frac{k_{io}}{1+k_{io}}T_{jb-1,k}+\frac{1}{1+k_{io}}T_{jb+1,k} \qquad r=r_b \qquad (17)$$

$$\frac{T_{J+1,k}-T_{J-1,k}}{2\Delta r}=-Bi\,T_{J,k} \qquad r=r_o \qquad (18)$$

$$T_{j,o}=T_{j,N} \qquad (19)$$

In Eqs. (15)-(19), Δr and $\Delta\theta$ are the increment in dimensionless space coordinates; $T_{j,k}$ is the dimensionless temperature of grid point (j,k) in which subscript j and k are the jth and kth grid point in r and θ coordinates, respectively; The subscript J and jb represent the grids at the outer surface, $r=r_o$, and at the boundary between the inner and outer layer wall, $r=r_b$, respectively. As shown in Eq. (17), $T_{jb,k}$ the dimensionless temperature at the boundary, can be represented by $T_{jb+1,k}$, the first point temperature of the outer layer wall in the radial direction, and $T_{jb-1,k}$, the last grid point temperature of the inner layer wall in the radial direction, so the temperature at the boundary in the grid can be eliminated from the calculation. Therefore, the successive matrix operation can be simplified. The governing equation and boundary condition Eqs. (15) - (19) for heat conduction can be re-arranged into a proper matrix equation; hence the temperatures for all grid points in the furnace wall can be obtained by only one calculation. The rearranged matrix equation with iterative form is shown as follows:

$$\mathbf{A}_{n\times n}\mathbf{T}_{n\times 1} = \mathbf{D}_{n\times 1} \tag{20}$$

where $\mathbf{A}$ is a constant matrix which is a function of the space increment Δr , $\Delta\theta$ and the system properties and can be constituted by a numerical method and a physical model; $\mathbf{T}$ is a column vector constituted by the dimensionless temperature field of the discrete points in the system, which is the dimensionless temperature field of all grid points in this work; Vector $\mathbf{D}$ is a function of the dimensionless boundary condition; and n is the number of linear equation groups after discretization. The chief aim of direct problem is to solve the dimensionless temperature field $\mathbf{T}$ for all grid points as the boundary condition and the heat property are known. Therefore, vector $\mathbf{T}$ in Eq. (20) is the unknown for solving in the direct problem. Its solution can be directly solved by the Gauss elimination method, and a small number of temperatures from the temperature field can be used as the measured temperatures for the inverse process.

B. The deterministic grey dynamic model

If a system consists of an input series $U^{(0)}(1)$, $U^{(0)}(2)$, … and an output series $X^{(0)}(1)$, $X^{(0)}(2)$, ….and the input series can affect the output series through a transfer function, then the system is a dynamic one. Through the transfer function the effect of the input series on the output series at some moment can continue to next several moments. The input series is called leading indicator by economists and the output series is the predicted series.

From the research by Box [9], the generalized model for describing continuous dynamic system can be written as:

$$(1+\xi_1 D+...+\xi_p D^p)X(t) = g(1+\eta_1 D+...+\eta_q D^q)U(t). \tag{21}$$

where D denotes d/dt ; ξ_p and η_q are constants; U and X are input and output series, respectively. This model is called transfer function model of (p,q) order.

For prediction by grey model GM(1,1), the original series should be treated by AGO. Its aim is to reduce the randomness of series. In this work a prediction method is proposed, which is called deterministic grey dynamic model, simply denotes as DGDM(1,1,1). In this model the grey differential equation GM(p,q) is replaced by the Eq.(21), the AGO of GM(p,q) is preserved, and the model parameters are estimated by using deterministic convergence scheme.

Assuming that $U^{(0)}$ and $X^{(0)}$ are input and output series of a dynamic system, and ($U^{(0)}(t)$, $X^{(0)}(t)$) can be obtained by means of observation at equal time intervals. For showing the relationship between variations of X and U, a prediction model DGDM(1,1,1) is established by the replacement of the U and X in Eq. (21) by series $U^{(1)}$ and $X^{(1)}$ formed from $U^{(0)}$ and $X^{(0)}$ through 1-AGO, respectively. In DGDM(1,1,1) the first 1 stands for the first-order derivative of 1-AGO series of $X^{(0)}$ series, the second 1 stands for the first-order derivative of 1-AGO series of $U^{(0)}$ series, and the third 1 stands for 1-AGO. Therefore, the grey dynamic model DGDM (1,1,1) can be written as:

$$R\frac{dX^{(1)}(t)}{dt} + X^{(1)}(t) = S_1\frac{dU^{(1)}(t)}{dt} + S_2 U^{(1)}(t) \ , \ t = 1,2,..,n \tag{22}$$

where,

$$X^{(1)}(t) = \sum_{i=1}^{t} X^{(0)}(i) \ , \ t = 1,2,...,n$$

$$U^{(1)}(t) = \sum_{i=1}^{t} U^{(0)}(i) \ , \ t = 1,2,...,n$$

They are the series formed from $X^{(0)}$ and $U^{(0)}$ by 1-AGO, respectively; R , S_1 and S_2 are the model parameters to be estimated. The first step for DGDM(1,1,1) is to estimate the model parameter R , S_1 and S_2 by deterministic convergence method. The $dX^{(1)}(t)/dt$ and $dU^{(1)}(t)/dt$ are obtained by fitting $X^{(1)}$ and $U^{(1)}$ to a cubic spline curve. The leading indicator $dU^{(1)}(t)/dt$ is further fitted by Fourier series and is integrated, and then the $U^{(1)}(t)$ is obtained. Finally, the $X^{(1)}(t)$ is solved and is operated by 1-IAGO to get $X^{(0)}(t)$, which is the prediction values of output series wanted by the present model.

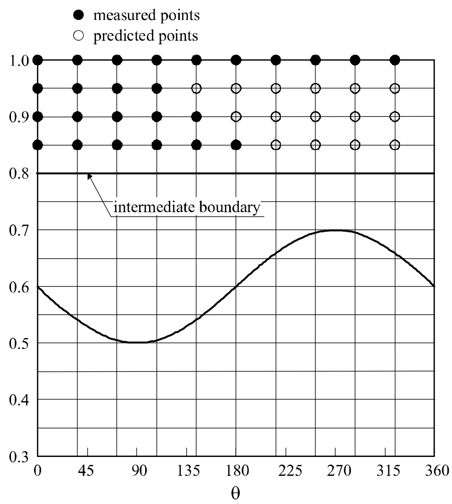

Fig.2 The schematic diagram for the locations of measured points and predicted points, and the calculated grid of a furnace wall with a sinusoidal inner surface.

To verify the appropriateness for application of DGDM(1,1,1) to the heat conduction problem, as shown in Fig.2, ten really measured temperatures at outer surface of furnace wall ($r = 1.0$) are taken as the leading indicator, $U^{(0)}(i)$, $i = 1,2,...,10$, and a prediction series taken from the temperatures at various measured locations under the case with a real measurement error, $\sigma = \pm 5\%$, for establishing DGDM(1,1,1). The predicted results are shown in table 1. It can be shown that the indirect measurement errors are larger than the real measurement errors when six points are predicted by prediction model established from four points data. This phenomenon can be ascribed to the number of predicted data larger than the number of data for establishing model and to the effect of real measurement error, which make the needed information insufficient and the system characteristics vague. When the number of data for establishing model is equal to or larger than the number of predicted data, the accuracy of prediction is still satisfactory even under the case with consideration of real measurement error. It is obvious from the results stated above that the temperatures obtained by DGDM(1,1,1) can be used as the measured temperatures for estimating the inner wall surface geometry of a two-layer-wall furnace in inverse process.

Table 1. The results predicted by DGDM(1,1,1) with a input series taken from the temperatures at outer surface of furnace wall ($r = 1.0$) and a prediction series taken from the temperatures at various measured locations under the case with a real measurement error, $\sigma = \pm 5\%$.

Prediction location r	Prediction grid point i	Indirectly measured value $\hat{X}^{(0)}(i)$	Really measured value $X^{(0)}(i)$	Error percentage of indirect measurement %
0.95	5	0.66981	0.65195	2.74
0.95	6	0.67520	0.67360	0.24
0.95	7	0.70204	0.77200	-9.06
0.95	8	0.67551	0.74632	-9.49
0.95	9	0.59882	0.71609	-16.38
0.95	10	0.51422	0.62700	-17.99
0.9	6	0.71521	0.68824	3.92
0.9	7	0.74263	0.77916	-4.69
0.9	8	0.77884	0.77618	0.34
0.9	9	0.72756	0.71459	1.82
0.9	10	0.70159	0.66861	4.93
0.85	7	0.77460	0.79090	-2.06
0.85	8	0.74383	0.73109	1.74
0.85	9	0.67409	0.70117	-3.86
0.85	10	0.63059	0.66026	-4.49

C. Inverse problem

In the inverse process for estimating the inner wall surface geometry of a two-layer-wall furnace, because the boundary geometry, $r_i(\theta)$, is unknown, the area for calculation cannot be sure so that the inverse process cannot be performed. Therefore the concept of virtual area is then introduced in this work. As shown in Fig.1, a virtual area is added in $r < r_i$ and some assumptions for this virtual area are made as follows. The virtual area has the same thermal conductivity, governing equation, basic assumption, and boundary conditions (except for the inner boundary of virtual area) as the actual system. Therefore, the inner boundary of virtual area can be changed as

$$T_{v,j} = T_d \qquad r = r_v \tag{23}$$

where, $r_v = 0.2$ is used in this work, the subscript v of $T_{v,j}$ denotes the grid point at the virtual boundary in the r direction; T_d is the temperature at the grid point (v, j) of the virtual boundary. For performing inverse operation, the governing equation and virtual boundary conditions would be rearranged, and the virtual system can be represented by the following matrix equation.

$$\mathbf{A}_{n\times n}\mathbf{T}_{n\times 1} = \mathbf{B}_{n\times m}\mathbf{C}_{m\times 1} \tag{24}$$

where, $\mathbf{A}$ is a constant matrix consisting of the thermal properties and space coordinates; $\mathbf{T}$ is a vector consisting of the temperatures of the measured points; vector $\mathbf{C}$ consists of temperature, $T_{d(v,j)}$, of the discrete points for determination; $\mathbf{B}$ is the coefficient matrix of $\mathbf{C}$; The n is the number of discretized linear equations; and m is the number of unknown boundary conditions.

The inverse model is then optimized by the linear least squares error method and the optimum of estimated value $\mathbf{C}_{est}$ can be got by solving following equation.

$$\mathbf{C}_{est} = (\mathbf{E}^T\mathbf{E})^{-1}\mathbf{E}^T\mathbf{T}_{mea} = \mathbf{R}\mathbf{T}_{mea} \tag{25}$$

where $\mathbf{E} = \mathbf{A}^{-1}\mathbf{B}$, $\mathbf{R} = (\mathbf{E}^T\mathbf{E})^{-1}\mathbf{E}^T$ is called the reverse matrix of the unknown boundary conditions. In sum, if measured value $\mathbf{T}_{mea}$ is given, the optimum of estimated value $\mathbf{C}_{est}$ can be obtained from the reverse matrix.

The main aim of the present work is to obtain the inner wall surface geometry of a two-layer-wall furnace. Using governing equation and boundary conditions consisting of the outer surface temperature of furnace wall and the estimated temperature of virtual boundary obtained from Eq.(25), the temperature field of furnace wall and virtual area can be simply solved by direct process. The isothermal line, $T(r,\theta) = 1$, in temperature field is just the inner wall surface geometry of a two-layer-wall furnace. It should be noticed that when the isothermal line does not lie on calculated grid points, the exact locations of isothermal line should be calculated by interpolation.

RESULTS AND DISCUSSION

It has been shown in section ***B*** that the results or the temperatures in furnace calculated by DGDM(1,1,1) is satisfactory. Hence the measured temperatures needed for inverse process can be taken partly from the really measured temperatures and partly from the indirectly measured temperatures obtained from a few of really measured temperatures through DGDM(1,1,1). To verify the appropriateness of the present method, it is necessary to discuss the effect of different numbers of measured points with different locations on the predicted result for the inner wall surface geometry of a two-layer-wall furnace.

In practice, the temperature measurement always contains some degree of error, of which magnitude depends upon the measuring method employed. Therefore, the simulated temperature measurement adopted in the inverse problem is also considered to include measurement errors. For reasons of practicality, the present study adds a random error noise to the exact temperature values computed from the direct problem. Hence, the measured dimensionless temperature, T_{mea}, is expressed as

$$T_{mea} = T_{exact}(1 + \sigma\omega) \tag{26}$$

where T_{exact} is the field temperature of the measured points obtained from the direct process, ω is a random number between -1 and 1, and σ is the standard deviation of the measurement error.

Fig.3 shows the temperature field of virtual area and furnace wall with a sinusoidal inner surface, which is obtained from four directly measured temperatures and six indirectly measured temperatures calculated by DGDM(1,1,1) at $r = 0.95$ under the case of neglecting measurement error. The isothermal line, $T(r_i, \theta) = 1$, in Fig.3 is just the inner wall surface geometry of a two-layer-wall furnace, which is what the present work wants. Above this isothermal curve is the furnace wall and below is the virtual area.

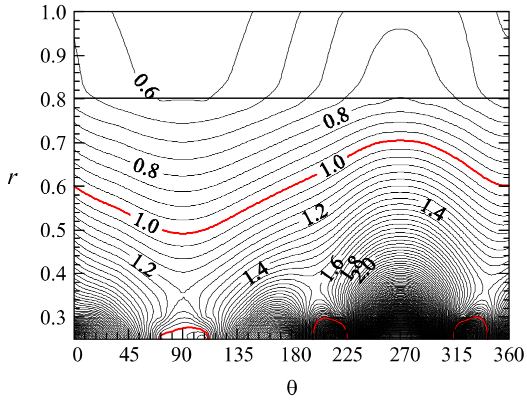

Fig.3 The temperature field of virtual area and furnace wall with a sinusoidal inner surface, which obtained from four directly measured temperatures and six indirectly measured temperatures calculated by DGDM(1,1,1) at $r = 0.95$ under the case of neglecting measurement error.

Fig.4 shows the results predicted from both temperatures of various measured points and indirectly measured temperatures calculated by DGDM(1,1,1) at $r = 0.95$ under the case with measurement error $\sigma = \pm 5\%$, the deviation of estimation for the inner surface geometry of furnace wall has an increasing trend due to the number of predicted points calculated by DGDM(1,1,1) not less than really measured points. When the number of predicted points calculated by DGDM(1,1,1) is less than the really measured points, the estimated result is then very consistent with the result (dotted curve) estimated without using DGDM(1,1,1)

For studying the effect of measurement error on the estimation of inner surface geometry of furnace wall, 10 grid points at $r = 0.95$ are selected, which consist of four points calculated by DGDM(1,1,1) and six really measured points, simply denoted DGDM(1,1,1)6-4. The grid points are so selected that the number of really measured points can be decreased and the accuracy of estimation is still preserved. The estimated results are shown in Fig.5 for the measurement error of $\sigma = \pm 1\%$, $\pm 3\%$ and $\pm 5\%$ respectively. For the case with measurement error $\sigma = \pm 1\%$, the estimated geometry has a slight deviation from the real values. The estimated values are also increased as measurement error increased to $\pm 3\%$ and $\pm 5\%$. However, the estimated geometry is still quite exact.

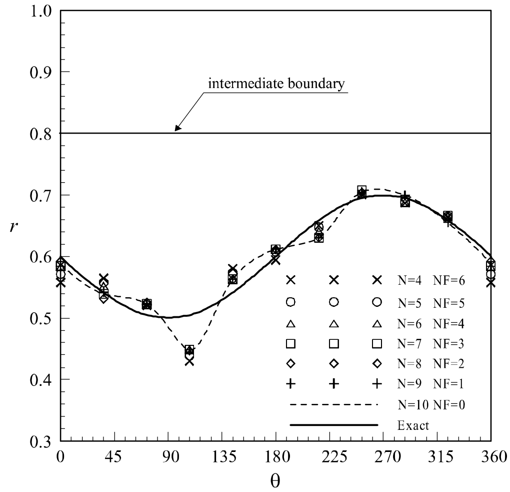

Fig.4 The inner surface geometry of furnace wall predicted from the temperatures of different measured points and the indirectly measured temperatures calculated by DGDM(1,1,1) at $r = 0.95$, $\sigma = \pm 5\%$ (N: number of measured points; NF: number of predicted points).

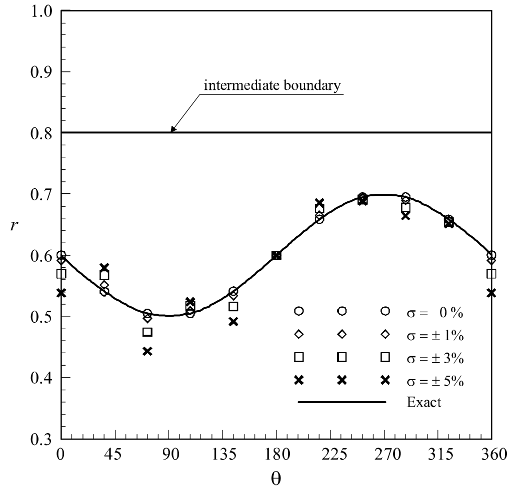

Fig.5 The effect of measurement error, $\sigma = 0\%$, $\pm 1\%$, $\pm 3\%$ and $\pm 5\%$, on the inner surface geometry of furnace wall estimated by DGDM(1,1,1)6-4 from measured points of $r = 0.95$.

Fig.6 shows the effect of measured point locations, $r = 0.95$, 0.90 and 0.85, on the estimation of inner surface geometry of furnace wall estimated by DGDM(1,1,1)6-4 for measurement error $\sigma = \pm 5\%$. It can be found that the estimated result is better for the measured points most near inner surface and the estimation deviation would increase with the increase of distance between the measured points and the boundary to be determined. For the thicker furnace wall at $45^\circ < \theta < 225^\circ$, the estimation deviation is obviously larger than other thinner furnace wall. These results display that the measured temperatures decrease as the measured points are farther from inner surface, in other words, the measurement error is an important factor for the estimation of inner surface geometry of furnace wall. In any case, the estimated result is still quite precise even for the measured locations much near outer surface.

For studying the effect of measured point number on the estimation of inner surface geometry, the inner surface geometry is first estimated by the values calculated by DGAM(1,1,1)6-4 at $r = 0.95$ for the measurement error $\sigma = \pm 5\%$. The estimated result is shown in Fig.7 It can be seen that the estimation deviation is relatively large for $45^\circ < \theta < 225^\circ$ due to the farther distance between measured points and boundary, and the other area has quite well estimated result. When a row of measured points are progressively added at $r = 0.90$ and $r = 0.85$, the result is obviously improved for the inner surface far removed from the measured points.:

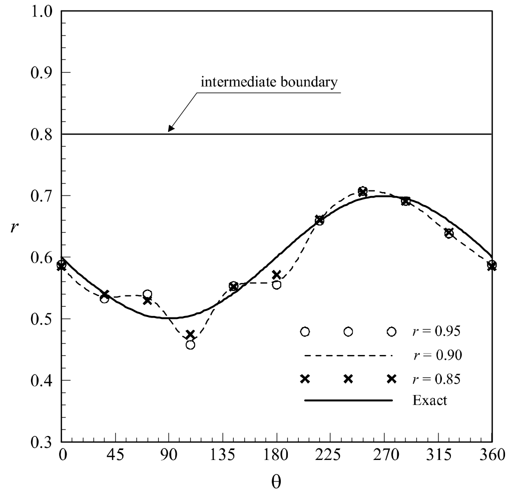

Fig.6 The effect of measured point location, $r = 0.95$, 0.90, and 0.85, on the inner surface geometry of furnace wall estimated by DGDM(1,1,1)6-4 for measurement error $\sigma = \pm 5\%$.

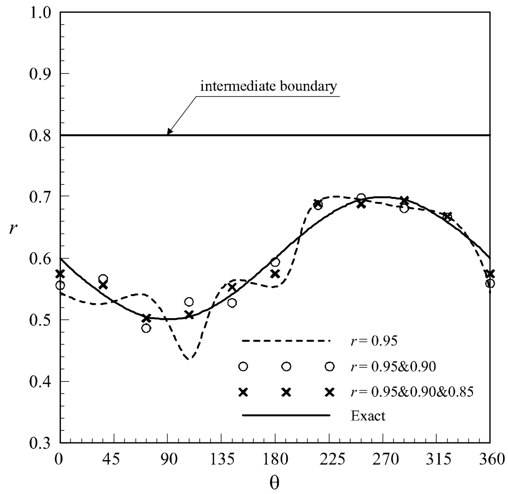

Fig.7 The effect of measured point number on the inner surface geometry of furnace wall estimated by DGDM(1,1,1)6-4 for measurement error $\sigma = \pm 5\%$.

CONCLUSIONS

In this work the inverse matrix method combined with DGDM(1,1,1) has been shown that it can be successfully used to estimate the inner wall surface geometry of a two-layer-wall furnace. It has advantages as follows. The unknown state to be estimated is first represented by a column vector and the estimated values can be obtained by only one operation process in which no assumptions are needed for the function form of unknown state, and the initially guessed values and iteration operation are also not necessary. It is quite efficient for treating unknown conditions with complexity. The accuracy of estimated values is increased with decrease in distance from measured points to the inner surface of furnace wall. In the case with relatively large measurement error, the accuracy of estimated values can be improved by increasing the number of measured points. In inverse process, the accuracy of estimation increases with increase in the number of measured points, and even in the case with a higher measurement error, the accuracy of estimation is still able to be preserved if the number of measured points is sufficient. Although the accuracy of estimation can be increased by the increase of measured points, the measurement cost is then increased and the efficiency is decreased accordingly. Therefore, the DGDM(1,1,1) can be combined to the inverse process to reduce the number of really measured points and still preserve the estimation accuracy. The method proposed in the present work can be applied to the academic and industrial circles.

ACKNOWLEDGMENT

The authors are grateful to the National Science Council of the Republic of China for supporting this research under grant. NSC 98-2221-E-150-054

REFERENCES

[1] J. H. Lin, C. K. Chen, Y.T. Yang, Inverse method for estimating thermal conductivity in one-dimensional heat conduction problems, *AIAA J. Thermo-physics and Heat Transfer*, 15(1), pp.34-41, 2001.

[2] H. Y. Jang, P. C. Tuan, T. C. Chen, T. S. Chen, Input estimation method combined with the finite-element scheme to solve IHCP hollow-cylinder inverse heat conduction problems, *Numerical Heat Transfer*, Part A, 50(3), pp263-280, 2006.

[3] C. K. Hsieh, A J.Kassab, A general method for the solution of inverse heat conduction problems with partially unknown system geometries, *Int. J. Heat and Mass Transfer*, 29(1), pp. 47-58, 1986.

[4] L. Met, X A. Wang, X Y. Meng, Finite element method to an inverse problem of three-dimensional heat conduction with partially unknown system geometries, *Proceedings of the Int. Conference on Numerical Methods in Thermal Problems*, pp.1514, 1991.

[5] C. H. Huang, B H. Chao, An Inverse Geometry Problem in identifying irregular boundary configurations, *Int. J. of Heat and Mass Transfer*, 40(9), pp.2045-2053, 1997.

[6] J. L. Deng, Control problems of grey systems, *Systems & Control Letters*, 1(5), pp.288-294, 1982.

[7] C. K. Chen, T.L. Tien, A new forecasting method of discrete dynamic system, *App. Math. and Comp.*, 86(1) pp.61-84, 1997.

[8] T.L. Tien, C. K. Chen, The indirect measurement of fatigue limits of structural steel by the deterministic grey dynamic model DGDM(1,1,1), *App. Math. Modeling*, 21(10), pp.611-619, 1997.

[9] G. E. P. Box, G. M. Jenkins, G. C. Reinsel, Time Series Analysis: Forecasting and Control, Prentice-Hall, New Jersey, 1994